In vivo tomographic velocimetry of the lung for the detailed study of lung disease and its treatments

Stephen Dubsky[a], Stuart B. Hooper[b], Karen K.W. Siu[c,d], Andreas Fouras*[a]

[a]Dept. Mechanical & Aerospace Engineering, Monash University, Clayton, VIC, AUS, 3800; [b]Monash Institute of Medical Research, Monash University, Clayton, VIC, AUS, 3800; [c]Monash Biomedical Imaging/School of Physics, Monash University, Clayton VIC, AUS, 3800; [d]Australian Synchrotron, 800 Blackburn Road, Clayton, VIC, AUS 3168

ABSTRACT

All lung disease dramatically alters the local motion of the lung during breathing. It stands to reason, therefore, that detailed measurement of lung motion could provide dramatic improvements in assessment of lung function. Using synchrotron-based phase contrast imaging, we have developed and applied tools for lung motion and function measurement. We demonstrate a low-dose alternative to traditional 4D-CT methods, capable of measuring instantaneous 3D tissue motion using only 6 projection images. Additionally, our technique provides estimation of the airflow distribution throughout the bronchial tree during the breathing cycle. The ability to measure lung function at a regional level will provide invaluable information for studies into normal and pathological lung dynamics, and may provide new pathways for diagnosis of regional lung diseases. Although proof-of-concept data were acquired on a synchrotron, the low-dose methodology developed lends itself to clinical scanning and offers translational opportunities.

Keywords: Computed tomography, functional imaging, lung, velocimetry, phase contrast, synchrotron

1. INTRODUCTION

Despite our rapidly increasing understanding of lung diseases, our ability to make further inroads into the treatment of diseases of the lung is critically limited by the lack of tools (at both the clinical and preclinical level) to measure lung function in a regional manner. For example, diagnoses may come too late because all too often, for a loss of total lung function to be measureable and thus clinically significant, local disease must be advanced. Since pulmonary function is normally measured at the mouth and hence averaged over the entire lung, current pharmacological treatments are developed and prescribed based on the global response of the lung. All lung pathologies cause significant regional changes in lung motion, and hence airflow, due to local changes in tissue compliance and/or resistance. Lung diseases such as emphysema, asthma and carcinoma are well known for the dramatic and heterogeneous alterations in lung properties they cause as well as the huge burden these diseases place on society.

Our ability to reduce the burden of lung diseases, including obstructive lung disease, is restricted by our inability to adequately image the lung. This is because all standard imaging modalities suffer significant problems when imaging the lungs. For instance, lung MRI signals are particularly weak and necessitate the use of expensive contrast gases. Also, the resolution is poor, with typical dimensions greater than 100 μm and scan times exceeding 5 seconds. Ultrasound signals are confounded by the lung's multiple airway cavities and image resolution is typically of the order of millimetres. X-ray imaging (plane radiography) is by far the most commonly used biomedical imaging modality. It is simple to use, has good spatial resolution and the resulting images are relatively easy to interpret. Unfortunately, conventional X-ray images display poor contrast for soft tissues such as the lungs.

*andreas.fouras@monash.edu; phone +61 3 9905-3493; ldi.monash.edu

Computed tomography (CT) has long been the gold standard for high-resolution medical imaging, and is typically performed using patient breath holds to reduce motion artifacts. Regional expansion can be measured by registration-based techniques[1,2,3,4] but information is typically inferred from static breath-hold images at the start and end of inspiration. Insufficient temporal resolution in high-resolution CT therefore hinders its ability to provide any information on the dynamics of pulmonary function. Clinical 4D (i.e. 3D + time resolved) CT techniques, which make use of respiratory gating, have been recently developed to dynamically image the human lung[5,6,7]. Nevertheless, the high X-ray dose delivered (a full CT dose per time point in the imaging sequence) severely reduces applicability of this method in the clinical setting. It has been demonstrated that lung disease can alter tissue motion dramatically, even in the subtle stages of disease[8]. Techniques that are capable of measuring the motion of the lung during breathing may therefore provide new diagnosis methods. Furthermore, these methods will aid in the assessment of the severity of disease, and the efficacy of existing and novel treatments.

We present here two variations of an imaging and analysis method capable of measuring *in vivo* motion and airflow within the lung, utilizing the advantages of synchrotron phase-contrast imaging. Synchrotron X-ray sources, due to their brightness and coherence, are able to provide dynamic, high-resolution imaging of the lung during breathing through the use of phase contrast imaging[9,10,11]. Lung tissue is an ideal sample for this technology, consisting of small air-filled sacs surrounded by soft tissue. This structure provides many air-tissue interfaces, which exhibit sharp refractive index gradients, on which the edge enhancement of phase contrast imaging is most effective.

In one approach, dynamic computed tomography provides a 4D image of the lung morphology. The motion of the lung can then be measured using a 3D correlation-based velocimetry method[12]. An alternative approach uses the method of Computed Tomographic X-ray Velocimetry (CTXV)[13,14]. This method is capable of directly reconstructing 3D motion fields directly from 2D cross-correlations derived from projection images. This approach can provide accurate tissue displacement information from a very low number of projections, resulting in significant reductions in radiation dose imparted to the sample. In the first application of CTXV to *in vivo* lung motion measurement, we present measurement of lung motion, derived from only 6 projection images (3 projection angles × 2 time-points).

A post-processing procedure is presented that can measure flow throughout the airway tree. By allocating regions of tissue to their corresponding supplying airways, the flow of air throughout the airways can be deduced[12].
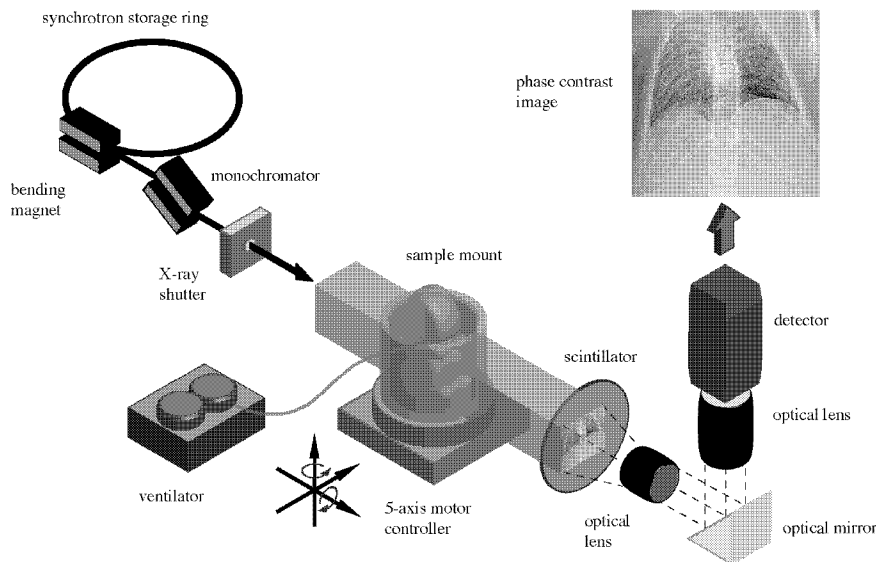

Figure 1. Schematic of synchrotron imaging setup. Monochromatic X-rays transmit through the sample onto a scintillator, which is imaged using an optical detector system. The animal, ventilated using a self-developed ventilator system, is positioned and aligned using a 5 axis robotic stage. A fast X-ray shutter is used for dose minimization. Modified from Dubsky *et al.* (2012)[12].

2. SYNCHROTRON PHASE CONTRAST IMAGING

Phase contrast images were acquired at the SPring-8 synchrotron, Japan. Figure 1 illustrates the experimental setup. X-rays are generated at the BL20B2 beam-line using a bending magnet insertion device. The X-ray beam then passes through a monochromator crystal (Si-111) tuned to deliver a monochromatic X-ray beam at 24 keV. An X-ray shutter is used to minimise the delivered radiation dose between image acquisitions. A large source-to-sample distance of ~210m ensures that the X-rays can be considered to be a parallel plane wave. Images were acquired using a Hamamatsu X-ray converter (BM5). The X-ray converter consists of a scintillator, and visible light detector (sCMOS). The X-rays transmit through the sample onto a scintillator (GADOX, $Gd2O2S:Tb+$, powder deposited, P43), which converts the X-ray photons into the visible spectrum for imaging with a visible light imaging system (Figure 1).

3. LUNG TISSUE MOTION AND EXPANSION MEASUREMENT

3.1 4DCT + cross correlation velocimetry

In one approach to motion measurement, dynamic computed tomography was used to acquire a 4D movie of the lung morphology. For details of the animal handling and analysis method, the reader is referred to Dubsky *et al.* (2012)[12]. Briefly, the animal is placed upright in a self-developed holder, which is mounted to a 5-axis motor controller. This allows precise alignment and rotation of the sample to reduce artifacts in the subsequent tomographic reconstructions. A custom designed ventilator, based on the device described in Kitchen *et. al* (2010)[15], provides stable, pressure-controlled ventilation, and provides triggering to the imaging system for synchronization with the ventilation cycle. Phase-contrast images are acquired as the sample is rotated through 180 degrees. Images from each time point are collated and reconstructed. Images first undergo a flat-dark correction, followed by single image phase retrieval[16]. An algebraic tomographic reconstruction was then performed at each time point to yield a 4D movie of the morphology of the lungs. A cross-correlation velocimetry approach is used to calculate the displacement of tissue regions between subsequent 3D image frames. This method is based on the discipline of particle image velocimetry (PIV). PIV is routinely used in fluid mechanics studies to accurately measure the velocity of tracer particles within a fluid flow, traditionally in two dimensions[17], but recently has been expanded to 3D[18]. The basic principle is as follows; corresponding regions (known as interrogation regions) of images acquired at a known time interval are cross-correlated. The position of the maximum in the correlation map will be equal to the most common inter-frame displacement of the particles within the interrogation region. Division of the displacement by the known interframe time interval yields velocity. Lung tissue is well suited to this form of analysis as it consists of many small airsacs, providing a high density of information with which to track the motion. In this way the airsacs act, in place of the particles, as motion tracers.
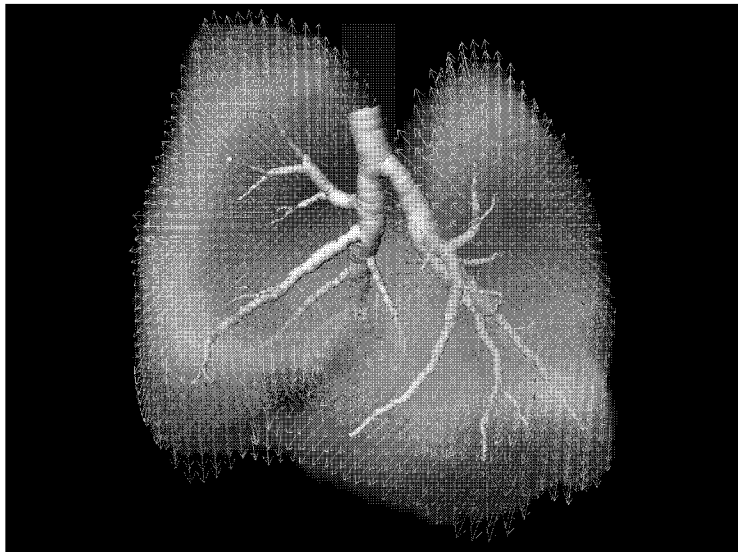

Figure 2. Lung tissue motion in a rabbit pup under mechanical ventilation. The arrows represent the displacement of the lung tissue over inspiration.

Figure 2 shows lung tissue motion of a newborn rabbit pup during mechanical ventilation. The arrows represent the displacement of lung tissue over the breath. Although this method is highly accurate and effective, it requires a single CT scan for each measured time-point (approximately 400 images per time point). This increases X-ray dose; a significant impediment to widespread clinical use.

3.2 Computed tomographic x-ray velocimetry

Computed tomographic x-ray velocimetry (CTXV) is a method capable of 3D measurement of motion fields from very few projection angles, originally developed for measurement of fluid flow[13,14]. The method reconstructs the 3D velocity field directly from 2D correlation functions calculated between regions of subsequent projection images. As the correlation functions contain much more information than a line integral, a reconstruction can be performed with far fewer projections than is required for traditional CT. The basic implementation described in Figure 3. Particle image pairs are discretized into interrogation regions, and cross correlation is performed on these regions. The resulting projected cross-correlation statistics can be modeled as the velocity probability density function (PDF) of the flow projected onto that sub-region of the image, convolved with the particle image auto-correlation function[19]. Therefore, if the flow field and particle image autocorrelation function are known, the cross-correlation functions that would theoretically result from the velocity field can be estimated.
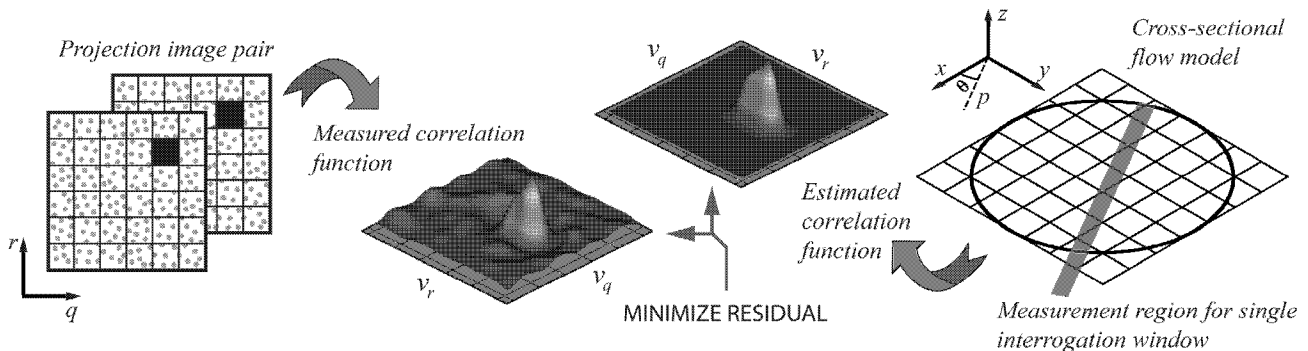

Figure 3. CTXV reconstruction. The residual between cross-correlation functions estimated from the flow model and those measured from the projection images is minimized over all interrogation windows and all projection angles simultaneously to yield a cross-sectional flow model that accurately represents the flowfield. From Dubsky et al. (2012)[14].

CTXV provides a solution for the inverse problem of reconstructing the flow field from the known cross-correlation data. The velocity field is reconstructed in slices orthogonal to the axis of rotation, concurrent with the rows of interrogation regions within the projection images. A rectangular grid model represents the velocity field in the reconstruction domain. The three velocity components are defined at each node point in the model, and bi-linear or spline interpolation is used to define the velocity between node points. A Levenberg–Marquardt algorithm is utilized to minimize the error between the cross-correlation functions estimated from the flow model and those measured from the projection image pairs, resulting in a calculated flow model that accurately represents the velocity-field.

We have successfully implemented CTXV for *in vivo* measurement of lung tissue motion from 6 projections (3 projection image pairs). Figure 4 shows the instantaneous velocity of lung tissue within a mouse during breathing, overlayed onto a CT dataset as an anatomical reference. The entire reconstruction (anatomy + velocity) was achieved with only 375 projections. Each motion measurement time-point requires an additional 3 images, resulting in an additional dose of only 0.8%. To reduce the dose further, it would be possible to generate the anatomical reference using an alternative imaging approach such as magnetic resonance imaging, resulting in an equivalent dose of only 6 plane-radiographs.
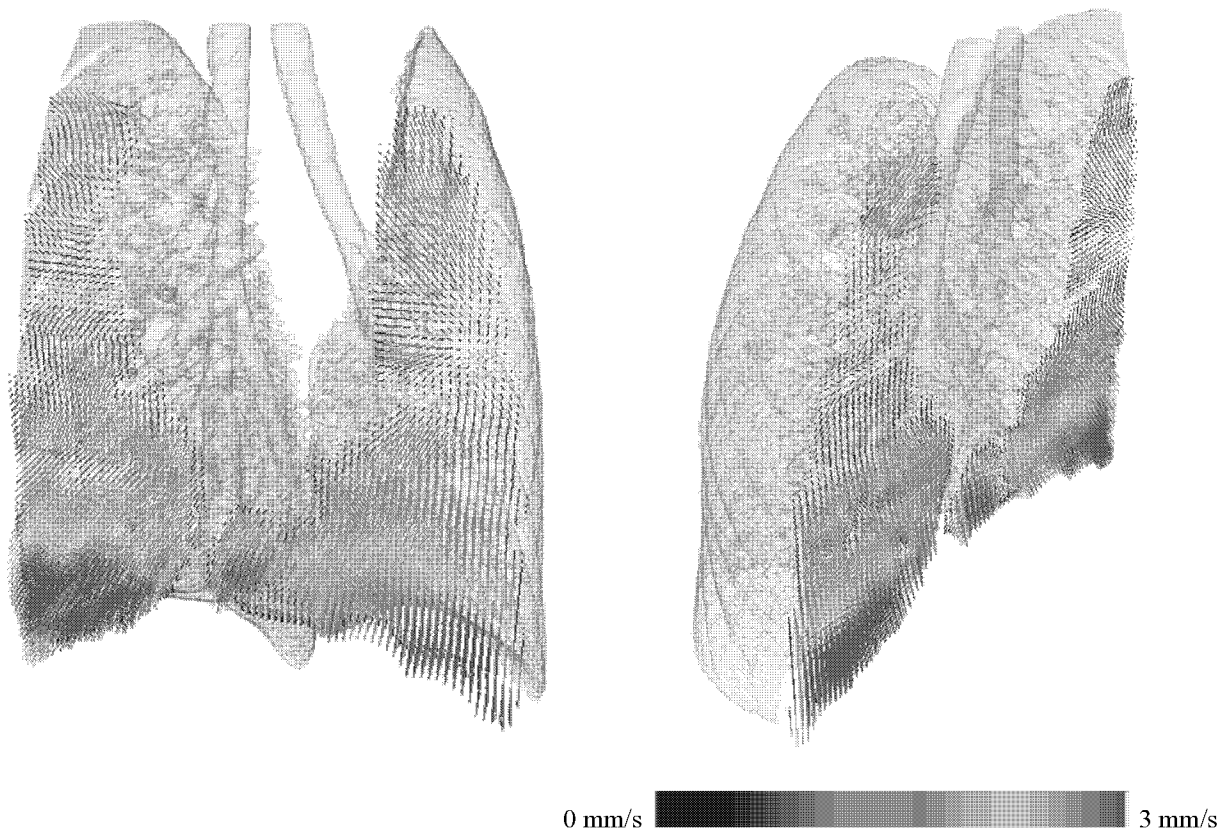
0 mm/s ▮▮▮▮▮▮▮▮▮▮▮▮▮▮▮▮▮▮ 3 mm/s

Figure 4. Instantaneous tissue velocity, measured using CTXV. Arrows represent the speed and direction of tissue velocity within a mouse during breathing, overlayed onto a CT dataset as an anatomical reference. The anatomical CT reconstruction was implemented with 375 projection images, and the motion measurement was achieved using 6 projection images (including 3 projections common to the CT reconstruction).

3.3 Tissue expansion calculation

Once the tissue motion field is known, the tissue expansion can be calculated as the divergence of the velocity field. Assuming that both the air inside the lung, and the tissue itself, is incompressible, the expansion calculated directly represents airflow into and out of these lung regions. The spatial partial derivatives were calculated using a two-step procedure: a polynomial is fitted to the velocity data via least-squares analysis, followed by analytic differentiation of the fitting polynomial[20]. Integration of the instantaneous expansion data with respect to time yields the change in volume from end expiration.

4. AIRWAY FLOW DISTRIBUTION

In order to relate the measured expansion field to airway flow, each region of tissue was associated with the airway that supplies that tissue. The entire procedure is illustrated in Figure 5. Since the tissue expansion results from flow into, or out of, the peripheral gas exchange airways, the airway flow is directly represented by the expansion of the tissue supplied by that airway. Each voxel was associated with its closest supplying airway. A supplying airway is defined as an airway that has a parent but no children. The airflow through each supplying airway can be directly inferred from the expansion of its associated tissue region. The mammalian bronchial tree is a dichotomous bifurcation network. The root is the trachea, and subsequent asymmetric bifurcations occur, with each airway (the parent), splitting into two daughter airways. Assuming negligible compressibility effects, the principle of continuity dictates that at each bifurcation the flow through a parent branch must equal to the sum of the flow through its daughter branches. Since the flow in each supplying airway is measured, the flow through the entire tree can therefore be calculated by recursively summing the flow rates in daughter branches at each bifurcation to calculate the parent branch flow rate.
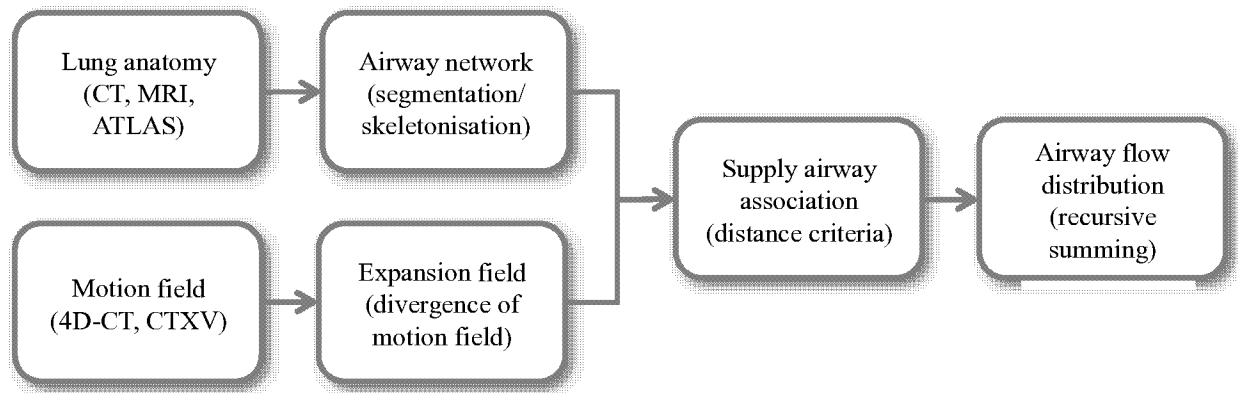
Figure 5. Flowchart of the flow measurement technique. Each voxel in the expansion field is associated with a supplying airway, allowing the flow through that airway to be deduced.

This method has been applied to the measurement of flow throughout the airway tree of a newborn rabbit pup (Figure 6). Airways were segmented from a CT reconstruction at the first time point. The airway segmentation procedure specified airways to 15 generations. Voxels in the expansion field were associated with their corresponding supplying airway to yield the flow throughout the airway tree for each time point imaged within the ventilation cycle.
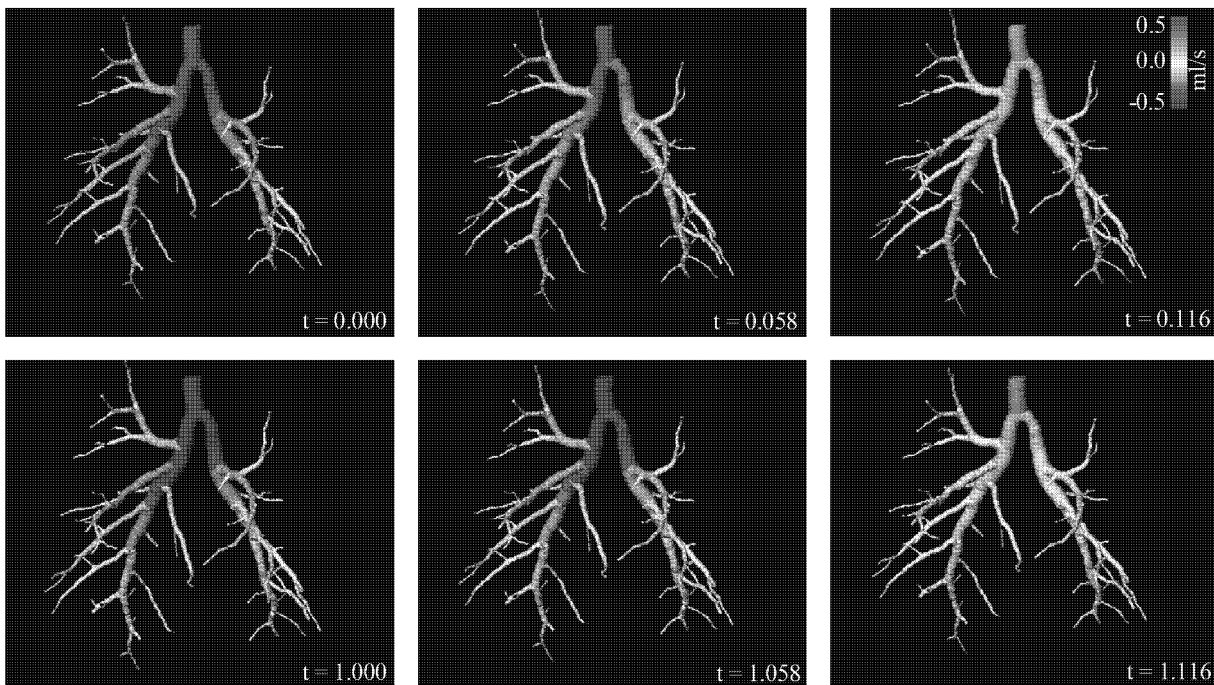

Figure 6. Distribution of flow throughout the airway tree. Instantaneous flow of air through the rabbit pup airway tree at six time points during ventilation. Positive flow indicates flow into the lungs and negative flow indicates flow out of the lungs. From Dubsky et al. (2012)[12].

5. CONCLUSIONS

We have presented methods for lung motion and function measurement. Measurement of tissue motion was achieved with only 6 projection images (3 projection angles × 2 time-points), providing dramatic reductions in dose when compared to 4D-CT based methods. The technique lends itself to evaluation of respiratory conditions in which there may be alteration in the compliance of lung, chest wall and diaphragmatic function or airway flow patterns. In particular, it may provide new insights into the regional consequences of restrictive lung disease, chronic obstructive airway diseases and asthma.

REFERENCES

[1]   Christensen, G.E., Song, J.H., Lu, W., El Naqa, I., and Low, D.A. "Tracking lung tissue motion and expansion/ compression with inverse consistent image registration and spirometry", Medical Physics, 34(6): p. 2155-2163, (2007).

[2]   Reinhardt, J.M., Ding, K. , Cao, K., Christensen, G.E., Hoffman, E.A., and Bodas, S.V. "Registration-based estimates of local lung tissue expansion compared to xenon CT measures of specific ventilation", Medical Image Analysis, 12(6): p. 752-763, (2008).

[3]   Yin, Y.B., Choi, J.W., Hoffman, E.A., Tawhai, M.H., and Lin, C.L. "Simulation of pulmonary air flow with a subject-specific boundary condition", Journal of Biomechanics, 43(11): p. 2159-2163, (2010).

[4]   Ding, K., Bayouth, J.E., Buatti, J.M., Christensen, G.E., and Reinhardt, J.M. "4DCT-based measurement of changes in pulmonary function following a course of radiation therapy", Medical Physics, 37(3): p. 1261-1272, (2010).

[5]   Guerrero, T., Sanders, K., Castillo, E., Zhang, Y., Bidaut, L., Pan, T.S., and Komaki, R. "Dynamic ventilation imaging from four-dimensional computed tomography", Physics in Medicine and Biology, 51(4): p. 777-791, (2006).

[6]   Pan, T., Lee, T.Y., Rietzel, E., and Chen, G.T.Y. "4D-CT imaging of a volume influenced by respiratory motion on multi-slice CT", Medical Physics, 31(2): p. 333-340, (2004).

[7]   Zhao, T.Y., Lu, W., Yang, D.S., Mutic, S., Noel, C.E., Parikh, P.J., Bradley, J.D., and Low, D.A. "Characterization of free breathing patterns with 5D lung motion model", Medical Physics, 36(11): p. 5183-5189, (2009).

[8]   Fouras, A., Allison, B., Kitchen, M., Dubsky, S., Nguyen, J., Hourigan, K., Siu, K., Lewis, R., Wallace, M., and Hooper, S. "Altered lung motion is a sensitive indicator of regional lung disease", Annals of Biomedical Engineering, 40(5), 1160–1169, (2012).

[9]   Hooper, S.B., Kitchen, M.J., Wallace, M.J., Yagi, N., Uesugi, K., Morgan, M.J., Hall, C., Siu, K.K.W., Williams, I.M., Siew, M., Irvine, S.C., Pavlov, K., and Lewis, R.A. "Imaging lung aeration and lung liquid clearance at birth", Faseb Journal, 21(12): p. 3329-3337,(2007).

[10]   Fouras, A., Kitchen, M.J., Dubsky, S., Lewis, R.A., Hooper, S.B. and Hourigan, K. "The past, present, and future of x-ray technology for in vivo imaging of function and form", Journal of Applied Physics, 105(10),(2009)

[11]   Lewis, R.A., Yagi, N., Kitchen, M.J., Morgan, M.J., Paganin, D., Siu, K.K.W., Pavlov, K., Williams, I., Uesugi, K., Wallace, M.J., Hall, C.J., Whitley, J., and Hooper, S.B. "Dynamic imaging of the lungs using X-ray phase contrast", Physics in Medicine and Biology, 50(21), p. 5031-5040 (2005).

[12]   Dubsky, S., Hooper, S., Siu, K.K.W., Fouras, A., "Synchrotron-based dynamic computed tomography of tissue motion for regional lung function measurement", Journal of the Royal Society Interface, 10.1098/rsif.2012.0116 (2012).

[13]   Dubsky, S., Jamison, R.A., Irvine, S.C., Siu, K.K.W., Hourigan, K., and Fouras, A. "Computed tomographic X-ray velocimetry", Applied Physics Letters, 96(2), (2010).

[14]   Dubsky, S., Jamison, R.A., Higgins, S., Siu, K.K.W., Hourigan, K & Fouras, A, "Computed tomographic X-ray velocimetry for simultaneous 3D measurement of velocity and geometry in opaque vessels", Experiments in Fluids, 52(3), p. 543–554, (2012).

[15] Kitchen, M. J., Habib, A., Fouras, A., Dubsky, S., Lewis, R. A., Wallace, M. J. & Hooper, S. B., "A new design for high stability pressure-controlled ventilation for small animal lung imaging", Journal of Instrumentation, 5, T02002 (2010).

[16] Irvine, S. C., Paganin, D. M., Dubsky, S., Lewis, R. A. & Fouras, A., "Phase retrieval for improved three-dimensional velocimetry of dynamic X-ray blood speckle", Applied Physics Letters, **93**, 153901 (2008).

[17] Adrian, R. J., "Particle-imaging techniques for exper- imental fluid-mechanics", Annual Review of Fluid Mechanics, **23**, p 261 – 304 (1991).

[18] Elsinga, G. E., Scarano, F., Wieneke, B. & van Oudheusden, B.W., "Tomographic particle image velocimetry", Experiments in Fluids, **41**, 933 – 947,(2006).

[19] Fouras, A., Dusting, J., Lewis, R., and Hourigan K., "Three-dimensional synchrotron x-ray particle image velocimetry.", Journal of Applied Physics, **102**(6), (2007).

[20] Fouras, A. & Soria, J., "Accuracy of out-of-plane vorticity measurements derived from in-plane velocity field data", Experiments in Fluids,**25**: p. 409 – 430 (1998).